The d^0, d^1 and d^2 Configurations in Known and Unknown Tetrathiometal Compounds MS_4^{n-} (M = Mo, Tc, Ru; W, Re, Os). A Quantum Chemical Study

Stanislav Záliš,[†] Hermann Stoll,[‡] Evert Jan Baerends,[§] and Wolfgang Kaim*,[⊥]

J. Heyrovský Institute of Physical Chemistry, Academy of Sciences of the Czech Republic, Dolejškova 3, CZ-18223 Prague, Czech Republic, Institut für Theoretische Chemie der Universität, Pfaffenwaldring 55, D-70550 Stuttgart, Germany, Afdeling Theoretische Chemie, Vrije Universiteit, De Boelelaan 1083, 1081 HV Amsterdam, The Netherlands, and Institut für Anorganische Chemie der Universität, Pfaffenwaldring 55, D-70550 Stuttgart, Germany

Received July 27, 1999

The known tetrathiometalates $MoS_4^{2-/3-}$, $WS_4^{2-/3-}$, $ReS_4^{-/2-/3-}$, and the unknown species $TcS_4^{-/2-}$, $RuS_4^{0/-}$, and $OsS_4^{0/-/2-}$ were calculated using ab initio and DFT methods. The one-electron reduced species with d^1 configuration were shown to exhibit a slight Jahn−Teller distortion ($T_d \rightarrow D_{2d}$); the largest corresponding stabilization energy was obtained for MoS_4^{3-} with −4.17 kcal/mol. Trends in vacuum bonding energies involve a destabilization on going from $5d^n$ to $4d^n$ systems and on reduction from d^0 to d^1 species, with the exception of Ru and Os complexes where the d^1 configurations are more stable than the d^0 forms. The d^2 species ReS_4^{3-} and OsS_4^{2-} have vacuum bonding energies similar to those of d^1 analogues. The metal contribution to the lowest unoccupied MO (e) of d^0 forms is lowest for the neutral RuS_4 and OsS_4 and highest for the dianions MoS_4^{2-} and WS_4^{2-}. The DFT approach supported by correlated ab initio calculations describes the main features of the electronic spectra of the d^0 complexes. For the experimentally best accessible ReS_4^{n-} system the absorption energies and stretching frequencies were well reproduced, and the related but hitherto unknown OsS_4^- ion is predicted to be a fairly stable paramagnetic species.

Tetrathiometalates MS_4^{n-} of the transition elements[1,2] with metal d^0 configuration (M = V, Nb, Ta and $n = 3$;[3] M = Mo, W and $n = 2$;[4] M = Re and $n = 1$)[4,5] have received attention in synthetic bioinorganic chemistry (precursors for models of Mo-[7] and W-containing enzymes[8,9]) and from catalysis where they serve as starting point for models directed at the improvement of hydrodesulfurization (HDS) catalysts for crude oil.[1,2,10−13] Under inorganic[4,11,15−20] and organometallic[21−30] aspects tetrathiometalates are interesting as potentially chelating, bridging, and cluster-forming components with relatively low-lying unoccupied d orbitals and high-lying sulfur-based molecular orbitals. Among the consequences of this situation are intense, low-energy ligand-to-metal charge transfer (LMCT) transitions; for the Mo^{VI}, W^{VI}, and Re^{VII} species these lie in the visible region.[4] Despite the relatively small HOMO−LUMO gaps, the reversible electrochemical reduction to d^1 species generally

[†] Academy of Sciences of the Czech Republic.
[‡] Institut für Theoretische Chemie der Universität.
[§] Vrije Universiteit.
[⊥] Institut für Anorganische Chemie der Universität.

(1) Stiefel, E. I., Matsumoto, K., Eds.; *Transition Metal Sulfur Chemistry*; American Chemical Society: Washington, DC 1996.
(2) Weber, T.; Prins, R.; van Santen, R. A., Eds.; *Transition Metal Sulphides—Chemistry and Catalysis*; NATO ASI Series; Kluwer Academic Publishers: Dordrecht, 1998.
(3) Lee, S. C.; Li, J.; Mitchell, J. C.; Holm, R. H. *Inorg. Chem.* **1992**, *31*, 1, 4333.
(4) Müller, A.; Diemann, E.; Jostes, R.; Bögge, H. *Angew. Chem.* **1981**, *93*, 957; *Angew. Chem., Int. Ed. Engl.* **1981**, *20*, 934.
(5) Müller, A.; Krickemeyer, E.; Bögge, H. *Z. Anorg. Allg. Chem.* **1987**, *554*, 61.
(6) Ciurli, S.; Carney, M. J.; Holm, R. H.; Papaefthymiou, G. C. *Inorg. Chem.* **1989**, *28*, 2696.
(7) Romão, M. J.; Huber, R. *Struct. Bonding* **1998**, *90*, 69.
(8) Johnson, M. K.; Rees, D. C.; Adams, M. W. W. *Chem. Rev.* **1996**, *96*, 2817.
(9) Hagen, W. R.; Arendsen, A. F. *Struct. Bonding* **1998**, *90*, 161.
(10) Chianelli, R. R.; Pecoraro, T. A.; Halbert, T. R.; Pan, W.-H.; Stiefel, E. I. *J. Catal.* **1984**, *86*, 226.
(11) McConnachie, E. A.; Stiefel, E. I. *Inorg. Chem.* **1999**, *38*, 964.
(12) Chianelli, R. R.; Daage, M., Ledoux, M. *Adv. Catal.* **1994**, *40*, 177.
(13) Topsøe, H.; Clausen, B. S.; Massoth, F. E. *Hydrotreating Catalysis: Science and Technology*; Springer-Verlag: Berlin, 1996.
(14) Müller, A.; Krickemeyer, E.; Wittneben, V.; Bögge, H.; Lemke, M. *Angew. Chem.* **1991**, *103*, 1501; *Angew. Chem., Int. Ed. Engl.* **1991**, *30*, 1512.
(15) Müller, A.; Krickemeyer, E.; Hildebrand, A.; Bögge, H.; Schneider, K.; Lemke, M. *J. Chem. Soc., Chem. Commun.* **1991**, 1685.
(16) Greaney, M. A.; Coyle, C. L.; Harmer, M. A.; Jordan, A.; Stiefel, E. I. *Inorg. Chem.* **1989**, *28*, 912.
(17) Wei, L.; Halbert, T. R.; Murray, III, H. H.; Stiefel, E. I. *J. Am. Chem. Soc.* **1990**, *112*, 6431.
(18) Gea, Y.; Greaney, M. A.; Coyle, C. L.; Stiefel, E. I. *J. Chem. Soc., Chem. Commun.* **1992**, 160.
(19) Lee, S. C.; Holm, R. H. *J. Am. Chem. Soc.* **1990**, *112*, 9654.
(20) Kony, M.; Bond, A. M.; Wedd, A. G. *Inorg. Chem.* **1990**, *29*, 4521.
(21) Howard, K. E.; Rauchfuss, T. B.; Rheingold, A. L. *J. Am. Chem. Soc.* **1986**, *108*, 297.
(22) Rosenhein, L. D.; McDonald, J. W. *Inorg. Chem.* **1987**, *26*, 3414.
(23) Howard, K. E.; Rauchfuss, T. B.; Wilson, S. R. *Inorg. Chem.* **1988**, *27*, 1710 and 3561.
(24) Howard, K. E.; Lockemeyer, J. R.; Massa, M. A.; Rauchfuss, T. B.; Wilson, S. R.; Yang, X. *Inorg. Chem.* **1990**, *29*, 4385.
(25) Unidentate ReS_4^- as a ligand: Massa, M. A.; Rauchfuss, T. B.; Wilson, S. R. *Inorg. Chem.* **1991**, *30*, 4667.
(26) Schäfer, R.; Kaim, W.; Fiedler, J. *Inorg. Chem.* **1993**, *32*, 3199.
(27) Kaim, W.; Hornung, F. M.; Schäfer, R.; Schwederski, B.; Fiedler, J. *Z. Anorg. Allg. Chem.* **1998**, *624*, 1211.
(28) Hornung, F. M.; Klinkhammer, K.-W.; Kaim, W. *J. Chem. Soc., Chem. Commun.* **1998**, 2055.
(29) Hornung, F. M.; Klinkhammer, K.-W.; Kaim, W. To be submitted.
(30) Kaim, W.; Schäfer, R.; Hornung, F. M.; Krejcik, M.; Fiedler, J.; Zalis, S. *Transition Metal Sulphides—Chemistry and Catalysis*; Weber, T., Ed.; NATO ASI Series; Kluwer Academic Publishers: Dordrecht, 1998; p 37.

10.1021/ic990891f CCC: $18.00
Published on Web 12/03/1999

occurs at rather negative potentials; for instance, we could show that very dry *N*,*N*-dimethylformamide (DMF) is necessary to observe reversible waves for the couple WS_4^{2-}/WS_4^{3-}.[27,31] The potentials for the reduction $d^0 \rightarrow d^1$ are least negative for the rhenium system $ReS_4^{-/2-}$.[6,26,32] Chelate coordination of additional metal electrophiles to MS_4^{n-} shifts the potential for the $d^0 \rightarrow d^1$ transition to less negative values;[30] in fact, trinuclear sulfido-bridged complexes $[L_nM(\mu\text{-}S)_2M(\mu\text{-}S)_2ML_n]^x$ with reduced MS_4^{n-} bridges were reported for $ML_n = FeCl_2$, $[Ru(bpy)_2]^{2+}$, $Mo(CO)_4$, $Mn(CO)_3Cl$, $Re(CO)_3Cl$, Cu(CN), and $PtPh_2$.[16,17,20,26,27,30−33]

The chemical persistence of the $Re^{VI}(5d^1)$ tetrathiometalate oxidation state at less negative potentials and the large electrochemical stability constant $K_c(ReS_4^{2-}) = 10^{\Delta E/0.059\ V} = 10^{14.9}$ raise the question whether other tetrathiometalates with d^1 configuration (or, for that matter, d^0 configuration) can be obtained. Since we had reported that WS_4^{2-} is reducible albeit at the very negative potential of $E[WS_4^{2-/3-}] = -3.16$ V vs $FeCp_2^{0/+}$ in dry DMF,[27,31] we have extrapolated in the $5d^1$ series via $E[ReS_4^{-/2-}] = -1.58$ V that the as yet unknown OsS_4^- should exist below $E \approx 0$ V vs $FeCp_2^{0/+}$; i.e., the paramagnetic Os^{VII} state may be a stable oxidation state in this form. Holm and co-workers, on the other hand, have proposed OsS_4^{2-} as a conceivable new tetrathiometalate.[3]

Herein we describe the use of quantum chemical methodology to calculate the properties of the known tetrathiometalates $MoS_4^{2-/3-}$, $WS_4^{2-/3-}$, $ReS_4^{-/2-/3-}$, and of the unknown species $TcS_4^{-/2-}$, $RuS_4^{0/-}$, and $OsS_4^{0/-/2-}$. Reliability of the calculations is checked through comparison with available experimental data. To calculate open shell forms such as OsS_4^-, we also had to consider d^1 species with potentially Jahn−Teller distorted ground states; the d^2 configuration was calculated for ReS_4^{3-} (which exists at very negative potentials)[6,26,32] and the unknown OsS_4^{2-}.

Calculation Procedures

Ground-state electronic structure calculations of MS_4^{n-} (M = Mo, Tc, Ru, W, Re, Os; $n = 0, 1, 2$) systems and their reduced states have been done by ab initio and time-dependent density functional theory (DFT) methods using the ADF-RESPONSE module[34] (an extension of Amsterdam density functional, ADF, program)[35] and Gaussian 98[36] program packages. The lowest excited states of closed shell complexes were calculated using the time-dependent DFT method (ADF-RESPONSE program) and complete active space SCF (CASSCF) method (MOLPRO 98 program).[37]

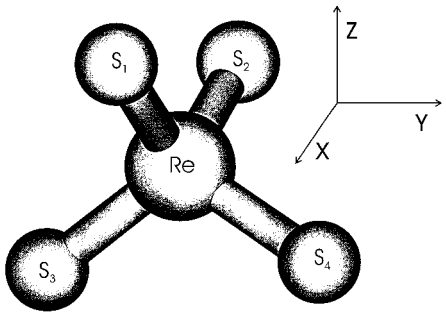

Figure 1. The ReS_4^- molecule with orientation of axes.

Within Gaussian 98 and MOLPRO Dunning's augmented correlation consistent valence double-ζ functions[38] were used for the S atoms and quasirelativistic pseudopotentials and corresponding optimized sets of basis functions for the metal atoms.[39] Becke's three-parameter hybrid functional with Lee, Yang, and Parr correlation part (G98-B3LYP)[40] was used in the Gaussian 98 calculations.

Within the ADF program Slater type orbital (STO) basis sets of triple-ζ quality with 3d polarization functions for S and additional p functions for the metals were employed. Inner shells were treated within the frozen core approximation (1s−2p for S, 1s−3d for Mo−Ru, and 1s−4d for W−Os). The following density functionals were used within ADF: local density approximation (LDA) with VWN parametrization of electron gas data and functionals including Becke's gradient correction[41] to the local exchange expression in conjunction with Perdew's gradient correction[42] to the LDA correlation (ADF-BP). The scalar relativistic (SR) zero-order regular approximation (ZORA)[43] was used in this study. The adiabatic local density approximation (ALDA) with the frequency dependence ignored was used in post-SCF time-dependent DFT calculations.

The ADF program exactly treats degeneracy in T_d (d^0 systems) and D_{2d} (d^1 systems) symmetry. Gaussian 98 and MOLPRO 98 use Abelian groups only; therefore, all calculations were done in constrained C_{2v} symmetry. The numbering of atoms and the Cartesian coordinate system of MS_4^{n-} complexes are depicted in Figure 1.

Results and Discussion

Molecular Orbitals. Calculated geometries and vacuum bonding energies for the d^0 and d^1 systems are summarized in Tables 1 and 2. Results from both the ADF-BP and G98-B3LYP functionals are shown (see below for a discussion of the differences).

The ADF-DFT calculated MO scheme for ReS_4^{n-} complexes in d^0 and d^1 configuration is depicted in Figure 2. Qualitatively

(31) Schäfer, R.; Fiedler, J.; Moscherosch, M.; Kaim, W. *J. Chem. Soc., Chem. Commun.* **1993**, 896.
(32) Schäfer, R.; Kaim, W.; Moscherosch, M.; Krejcik, M. *J. Chem. Soc., Chem. Commun.* **1992**, 834.
(33) Müller, A.; Krickemeyer, E.; Baumann, F.-W.; Jostes, R.; Bögge, H. *Chimia* **1986**, *40*, 310.
(34) van Gisbergen, S. J. A.; Snijders, J. G.; Baerends E. J.; with contributions by Groeneveld, J. A.; Koostra, F.; Osinga, V. P. *RESPONSE, extension of ADF program for linear and nonlinear response calculations*, ADF 2.3.0; Theoretical Chemistry, Vrije Universiteit, Amsterdam.
(35) te Velde, G.; Baerends, E. J. *J. Comput. Phys.* **1992**, *99*, 84.
(36) Frisch, M. J.; Trucks, G. W.; Schlegel, H. B.; Scuseria, G. E.; Robb, M. A.; Cheeseman, J. R.; Zakrzewski, V. G.; Montgomery, Jr., J. A.; Stratmann, R. E.; Burant, J. C.; Dapprich, S.; Millam, J. M.; Daniels, A. D.; Kudin, K. N.; Strain, M. C.; Farkas, O.; Tomasi, J.; Barone, V.; Cossi, M.; Cammi, R.; Mennucci, B.; Pomelli, C.; Adamo, C.; Clifford, S.; Ochterski, J.; Petersson, G. A.; Ayala, P. Y.; Cui, Q.; Morokuma, K.; Malick, D. K.; Rabuck, A. D.; Raghavachari, K.; Foresman, J. B.; Cioslowski, J.; Ortiz, J. V.; Stefanov, B. B.; Liu, G.; Liashenko, A.; Piskorz, P.; Komaromi, I.; Gomperts, R.; Martin, R. L.; Fox, D. J.; Keith, T.; Al-Laham, M. A.; Peng, C. Y.; Nanayakkara, A.; Gonzalez, C.; Challacombe, M.; Gill, P. M. W.; Johnson, B.; Chen, W.; Wong, M. W.; Andres, J. L.; Gonzalez, C.; Head-Gordon, M.; Replogle, E. S.; Pople, J. A. *Gaussian 98*, Revision A.6; Gaussian, Inc.: Pittsburgh, PA, 1998.
(37) Werner, H.-J.; Knowles, P. J. with contributions from Amos, R. D.; Berning, A.; Cooper, D. L.; Deegan, M. J. O.; Dobbyn, A. J.; Eckert, F.; Hampel, C.; Leininger, T.; Lindh, R.; Lloyd, A. W.; Meyer, W.; Mura, M. E.; Nicklass, A.; Palmieri, P.; Peterson, K.; Pitzer, R.; Pulay, P.; Rauhut, G.; Schütz, M.; Stoll, H.; Stone, A. J.; Thorsteinsson, T. *MOLPRO 98.1*.
(38) Woon, D. E.; Dunning, Jr., T. H. *J. Chem. Phys.* **1993**, *98*, 1358.
(39) Andrae, D.; Haeussermann, U.; Dolg, M.; Stoll, H.; Preuss, H. *Theor. Chim. Acta* **1990**, *77*, 123.
(40) Stephens, P. J.; Devlin, F. J.; Cabalowski, C. F.; Frisch, M. J. *J. Phys. Chem.* **1994**, *98*, 11623.
(41) Becke, A. D. *Phys. Rev. A* **1988**, *38*, 3098.
(42) Perdew, J. P. *Phys. Rev. A* **1986**, *33*, 8822.
(43) van Lenthe, E.; Baerends, E. J., Snijders, J. G. *J. Chem. Phys.* **1994**, *101*, 9783.

Table 1. Calculated Parameters of MS_4^{n-} Complexes in d^0 Configuration[a]

	MoS_4^{2-}	TcS_4^-	RuS_4	WS_4^{2-}	ReS_4^-	OsS_4
r_{M-S} (Å)/B3LYP	2.221	2.160	2.116	2.235	2.169	2.134
r_{M-S} (Å)/BP	2.240	2.171	2.133	2.242	2.183	2.139
r_{M-S} (Å)/expt	2.177	−	−	2.178	2.155	−
$\nu(t_2)$ (cm^{-1})/B3LYP	461.8	−	513.8	439.3	488.2	502.6
$\nu(t_2)$ (cm^{-1})/BP	448.3	491.8	502.7	425.0	473.8	492.7
$\nu(t_2)$ (cm^{-1})/expt	455	−	−	458	490	−
bonding energy (kcal/mol)/B3LYP	−424.4	−437.2	−311.8	−476.0	−463.9	−357.6
bonding energy (kcal/mol)/BP	−464.7	−494.6	−376.0	−530.6	−515.5	−431.8

[a] T_d symmetry.

Table 2. Calculated Parameters of Reduced MS_4^{n-} Complexes (d^1 Configuration, $^2A_1$ State)

	MoS_4^{3-}	TcS_4^{2-}	RuS_4^-	WS_4^{3-}	ReS_4^{2-}	OsS_4^-
r_{M-S} (Å)/B3LYP	2.305	n.o.[a]	2.153	2.313	2.223	2.173
α_1/B3LYP	110.25	n.o.	109.71	110.26	109.87	109.59
α_2/B3LYP	108.02	n.o.	109.37	107.92	108.68	109.24
ν(e) (cm^{-1})/B3LYP	374.7	n.o.	458.2	383.1	437.2	459.3
$\nu(b_2)$ (cm^{-1})/B3LYP	400.2	n.o.	480.4	361.2	421.2	470.4
ν (cm^{-1})/expt	n.a.[b]	−	−	n.a.[b]	439	−
bonding energy (kcal/mol)/B3LYP	−260.9	n.o.	−387.3	−303.0	−409.2	−428.2
bonding energy (kcal/mol)/ BP	−301.8	−443.2	−445.2	−359.4	−461.0	−493.1
E_{JT} (kcal/mol)/BP	−4.17	−2.76	−1.76	−3.80	−2.56	−1.83
spin density on M /B3LYP	0.920	n.o.	0.460	0.911	0.721	0.462

[a] The geometry optimization using G98 does not converge to stationary point. [b] Not available.

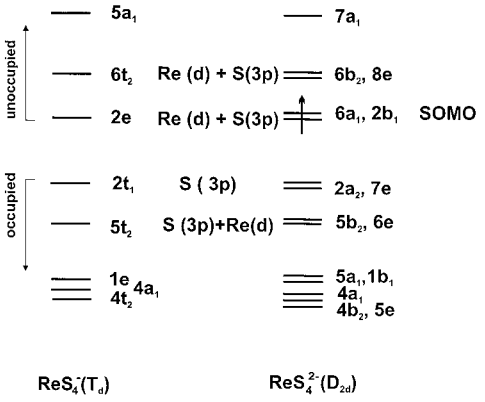

Figure 2. Molecular orbital scheme for ReS_4^- and ReS_4^{2-} ions calculated by the ADF method. The MO scheme for ReS_4^{2-} corresponds to spin-restricted calculation. The HOMOs of the ReS_4^- and ReS_4^{2-} complexes are set at the same energy value.

similar MO pictures are obtained for all systems studied, independently of the method used. The valence sphere of Mo − Ru does not contain 4f electrons. Therefore, the numbering of molecular orbitals differs from that in ReS_4^-; e.g., levels $1t_1$ and $4t_2$ form the set of the highest MOs in the case of MoS_4^{2-}, TcS_4^-, and RuS_4.

The highest occupied orbital (HOMO) of all d^0 complexes examined is the ligand localized t_1, formed by 3p (S) orbitals. The lower lying t_2 MO (HOMO−1) is a ligand localized orbital with small contributions of less than 12% from the central metal atom. The lowest unoccupied molecular orbital (LUMO, e) is to a large extent formed by d_{z^2} and $d_{x^2-y^2}$ orbitals of the central atom. The next unoccupied MO (LUMO+1), t_2 also has a large metal contribution. Nevertheless, the DFT calculations show a remarkable contribution from sulfur p orbitals to these unoccupied MOs. The composition of the e orbital (LUMO) is summarized in Table 3. This table shows strongly diminished metal contribution and thus increased orbital mixing on decreasing negative charge of the complexes, for both the 4d and 5d homologues. Although the best accessible d^1 species ReS_4^{2-} did not exhibit an EPR signal[32] due to very close lying states as a result of Jahn−Teller distortion (cf. below), the calculated

Table 3. Composition of the Lowest Unoccupied Molecular Orbital (e) Calculated by ADF and Gaussian 98 (Metal Character (%) in E MO)

DFT functional	MoS_4^{2-}	TcS_4^-	RuS_4	WS_4^{2-}	ReS_4^-	OsS_4
B3LYP	65.6	51.1	38.4	70.1	50.7	40.2
BP	47.8	38.1	30.1	49.1	37.7	29.1

result of 37.7% (BP) or 50.7% (B3LYP) metal particiation at the LUMO is confirmed by EPR spectroscopy of derivatives.[32]

Geometry. The geometry optimization of all d^0 systems leads to a tetrahedral arrangement. The G98-B3LYP and ADF-BP calculated M−S bond lengths are listed in Table 1. G98-B3LYP calculated bond lengths are in agreement with previously published[44] ab initio results for a number of related transition metal chalcogenides. In those cases where the experimental structure is known, the calculated bond lengths are slightly overestimated. ADF-BP calculated M−S bond lengths are by ∼0.015 Å longer than those calculated with the G98-B3LYP functional. In agreement with previous work on Werner-type complexes[45] and RuO_4^{n-} systems,[46] ADF calculations using the BP functional overestimate bond distances; ADF-LDA calculated bond lengths are close to those calculated using the G98-B3LYP functional.

During the reduction process the added electron is accepted by a degenerate e MO. The resulting ^2E state of the d^1 system is Jahn−Teller (JT) active which leads to distortion of the T_d symmetry. Lowering of symmetry causes the e MO to split into an a_1 and b_1 orbital. A compressed D_{2d} arrangement then corresponds to a $^2A_1$ state, the elongated one to a $^2B_1$ state (Figure 3). The composition of the redox orbital does not substantially change during the reduction process.

Further reduction leads to a d^2 configuration where the resulting $^3B_1$ state (in D_{2d} symmetry) is not Jahn−Teller active.

The optimized geometry of the d^1 complexes calculated by the spin-unrestricted DFT method is Jahn−Teller perturbed,

(44) Benson, M. T.; Cundari, T. R.; Lim, S. J.; Nguyen, H. D.; Pierce-Beaver, K. *J. Am. Chem. Soc.* **1994**, *116*, 3955.
(45) Bray, M. R.; Deeth, R. J.; Paget, V. J.; Sheen, P. D. *Int. J. Quantum Chem.* **1996**, *61*, 85.
(46) Deeth, R. J. *J. Chem. Soc., Dalton Trans.* **1995**, 1537.

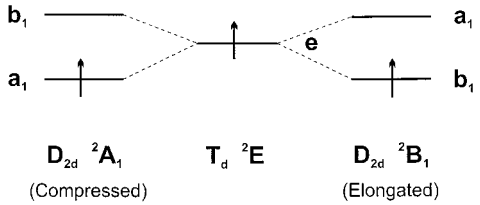

Figure 3. Qualitative description of e MO splitting due to the Jahn−Teller distortion $T_d \rightarrow D_{2d}$ (for choice of axes see text).

corresponding to D_{2d} symmetry. D_{2d} symmetry is characterized by equidistant M−S bond lengths and two different S−M−S angles α_1 (S_1-M-S_2 and S_3-M-S_4) and α_2 (angles formed between any S atom lying above and any S atom lying under the *xy* plane) (Figure 1). Two slightly different geometries result for forms compressed ($\alpha_1 > \alpha_2$) or elongated ($\alpha_1 < \alpha_2$) along the *z* axis. Table 2 shows that the addition of an electron into a_1 MO causes a lengthening of the M−S bonds in comparison with corresponding d^0 species. The distortion of the T_d structure depends on the metal character of redox orbital; therefore, the difference $\alpha_1 - \alpha_2 = \Delta\alpha$ increases from RuS_4^- to MoS_4^{3-} and from OsS_4^- to WS_4^{3-}. The qualitatively similar results are obtained for $^2B_1$ state.

The Jahn−Teller stabilization energy (E_{JT}) is calculated according to described[46,47] procedures as the difference between the total energy of the JT perturbed system and the energy of the system optimized within T_d symmetry constraints. This calculation was done using the ADF program. The largest stabilization energy, −4.17 kcal/mol, is obtained for the MoS_4^{3-} complex. As with the $\Delta\alpha$ distortion, E_{JT} correlates with the metal contribution to the corresponding redox orbital; nevertheless, the absolute degree of distortion remains fairly small ($\Delta\alpha < 2.5°$).

The geometry optimization of ReS_4^{3-} and OsS_4^{2-} complexes was performed using the ADF-BP method. The optimization leads to the T_d symmetry. Calculated M−S bond lengths are 2.293 and 2.217 Å for ReS_4^{3-} and OsS_4^{2-}, respectively, considerably lengthened compared with the corresponding d^1 systems.

Bonding Energies. The bonding energies listed in Table 1 were calculated at optimized geometry. Bonding energies are defined as the energy lowering of the molecular system with respect to the isolated constituent atoms, and their calculation requires a correct description of atomic multiplets. The values in Table 1 are based on atomic calculations for the following multiplets: Mo ($4d^55s^1 - {}^7S$), Tc ($4d^55s^2 - {}^6S$), Ru ($4d^75s^1 - {}^5F$), W ($5d^46s^2 - {}^5D$), Re ($5d^56s^2 - {}^6S$), Os ($5d^66s^2 - {}^5D$) and S ($3s^23p^4 - {}^3P$).

G98-B3LYP calculated bonding energies are based on spin-unrestricted atomic calculations without use of symmetry. The reliability of G98-B3LYP calculated atomic energies was checked by independent MOLPRO98 calculations in D_{2h} symmetry. The test MOLPRO98 B3LYP calculation on ReS_4^- gives the bonding energy at −463.7 kcal/mol, which is close to the −463.9 kcal/mol from G98-B3LYP calculations (Table 1). The ADF-BP calculated atomic bonding energies are based on ground-state energies of spherically symmetric spin-polarized atoms.[48] BP calculated bonding energies are lower than B3LYP ones; nevertheless, the trends of bonding energies within the triads of metals are similar and the calculated bonding energies

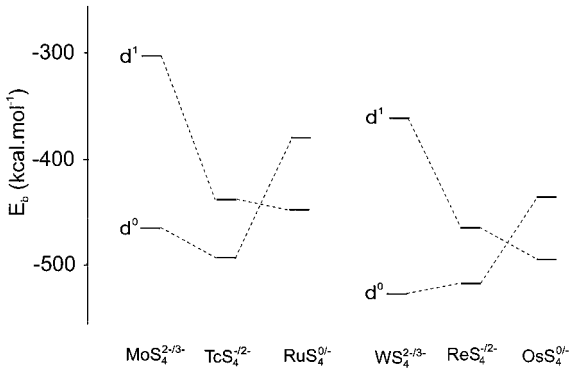

Figure 4. ADF-BP-calculated vacuum bonding energies of MS_4^{n-} species.

can indicate the relative stability of individual complexes examined. Figure 4 illustrates the changes in ADF-BP bonding energies on reduction and metal variation.

The ADF-BP calculated bonding energy of OsS_4^{2-}, −453.1 kcal/mol, lies between values calculated for d^0 and d^1 species. Due to the calculated bonding energy of −309.9 kcal/mol the ReS_4^{3-} complex should be more stable than MoS_4^{3-}.

The calculated bonding energies correspond to the molecular systems in a vacuum. In the real environment, the negatively charged systems can be stabilized either by the solvent or by counterions (lattice effects).

Molecular Vibrations. The vibrational analysis of MS_4^{n-} systems based on DFT wave functions produces the IR-active t_2 vibrations listed in Table 1. The experimental values for MoS_4^{2-}, WS_4^{2-}, and $ReS_4^{-/2-}$ are well reproduced by the calculated frequencies. For reduced system MS_4^{n-} with d^1 configuration the shift to lower frequencies is predicted as was observed for the $ReS_4^{-/2-}$ couple.[32] Due to the lower symmetry, D_{2d}, the allowed t_2 vibrations splits into e and b_2 features. ADF-BP calculated frequencies are shifted to lower values in comparison with those calculated using the G98-B3LYP functional.

Electronic Transitions. It has long been acknowledged that the lowest lying excited states of the d^0 complexes have LMCT character and arise by excitation from the ligand localized occupied t_1 and t_2 MOs to unoccupied metal localized MOs.[4,49] Both TD DFT and CASSCF calculations show a large coupling of states formed by excitation from the ligand based t_1 MO with those formed by excitation from t_2 into the virtual orbitals. Therefore, the electronic spectra of these complexes cannot be explained by individual one-electron transitions only.

The BP/ALDA symmetry-allowed T_2 excitation energies and oscillator strengths calculated for MoS_4^{2-}, WS_4^{2-} and ReS_4^- are compared with experimentally measured transitions in Table 4.

This table shows that the time-dependent DFT method well reproduces the characteristic features of electronic spectra of MS_4^{n-} complexes. The composition of individual excitations in terms of major one-electron transitions points to the possible mixing of one-electron excitations. In the visible to near-ultraviolet part of the electronic spectra of all complexes two $^1A_1 \rightarrow {}^1T_2$ transitions with relatively large oscillator strengths are calculated in agreement with the experiment. Also, the

(47) Bruyndonc, R.; Daul, C.; Manoharan, P. T.; Deiss, E. *Inorg. Chem.* **1997**, *36*, 4251.
(48) Baerends, E. J.; Branchadell, V.; Sodupe, M. *Chem. Phys. Lett.* **1997**, *265*, 481.
(49) See MO diagrams in: (a) Bernholc, J.; Stiefel, E. I. *Inorg. Chem.* **1985**, *24*, 1323. (b) Green, J. C.; Guest, M. F.; Hillier, I. H.; Jarrett-Sprague, S. A.; Kaltsoyannis, N.; MacDonald, M. A.; Sze, K. H. *Inorg. Chem.* **1992**, *31*, 1588. (c) Müller, A.; Jostes, R.; Schmitz, K.; Krickemeyer, E.; Bögge, H.; Bill, E.; Trautwein, A. *Inorg. Chim. Acta* **1988**, *149*, 9.

Table 4. Calculated TD DFT Transition Energies (eV) for Tetrathiometalates

complex	state	composition	transition energy	oscillator strength	expt transition[a]
MoS_4^{2-}	$^1T_2$	89%($1t_1 \rightarrow 2e$)	2.67	0.026	2.61[b] (12 880)
$^1T_2$	37%($4t_2 \rightarrow 2e$), 38%($1t_1 \rightarrow 5t_2$)		2.66	<0.001	
$^1T_2$	37%($4t_2 \rightarrow 2e$), 38%($1t_1 \rightarrow 5t_2$), 8%($4t_2 \rightarrow 5t_2$)		4.06	0.032	3.85[b] (17 780)
$^1T_2$	74%($4t_2 \rightarrow 5t_2$)		4.88	0.008	
WS_4^{2-}	$^1T_2$	88%($2t_1 \rightarrow 2e$)	2.86	0.030	3.12[b] (18 620)
$^1T_2$	40%($5t_2 \rightarrow 2e$), 32%($2t_1 \rightarrow 6t_2$)		3.70	0.002	
$^1T_2$	40%($5t_2 \rightarrow 2e$), 32%($2t_1 \rightarrow 6t_2$), 9%($5t_2 \rightarrow 6t_2$)		4.22	0.043	4.41[b]
$^1T_2$	74%($5t_2 \rightarrow 6t_2$)		5.24	0.160	
ReS_4^-	$^1T_2$	88%($2t_1 \rightarrow 2e$), 4%($2t_1 \rightarrow 6t_2$)	2.39	0.020	2.43[c] (12 700)
$^1T_2$	24%($5t_2 \rightarrow 2e$), 36%($2t_1 \rightarrow 6t_2$)		3.23	0.001	
$^1T_2$	24%($5t_2 \rightarrow 2e$), 36%($2t_1 \rightarrow 6t_2$), 25%($5t_2 \rightarrow 6t_2$)		4.02	0.042	3.96[c] (24 300)
$^1T_2$	66%($5t_2 \rightarrow 6t_2$)		5.16	0.144	

[a] In acetonitrile solution; molar extinction coefficients ϵ (M^{-1} cm^{-1}) in parentheses. [b] From ref 4. [c] From ref 32.

changes related to central atom variation are reproduced. The first allowed transition can be described as a HOMO to LUMO transition. The second allowed transition is mainly expressed as a combination of HOMO−1 to LUMO and HOMO to LUMO+1 one-electron excitations.

CASSCF calculations were done in C_{2v} symmetry, and therefore six nondegenerate orbitals corresponding to the t_1 and t_2 highest occupied orbitals have to be included in active space together with five unoccupied nondegenerate orbitals, corresponding to the lowest unoccupied e and t_2 levels. Thus, the direct product $T_1 \otimes E$ gives two triply degenerate representations T_1 and T_2; any t_1 (t_2) → e excitation produces two triply degenerate states. To preserve the degeneracy of all states, it is necessary to calculate simultaneously a proper number of state-averaged roots. In the following second-order perturbation calculations (CASPT2),[50] CASSCF wave functions were used as references.

In the CASSCF calculation on ReS_4^- 12 electrons were correlated within active space composed of 11 nondegenerate orbitals corresponding to the highest occupied t_1 and t_2 and lowest unoccupied e and t_2 levels. The simultaneous calculation of 15 state-averaged roots satisfactorily describes the degeneracy of individual states. The CASPT2 calculation gives a qualitatively good description of the electronic spectra (two allowed $^1A_1 \rightarrow {}^1T_2$ transitions) but overestimates the transition energies. In agreement with TD DFT, the first allowed transition calculated at 2.85 eV can be characterized as a HOMO to LUMO transition. The second one (calculated at 3.71 eV) cannot be assigned to any specific one-electron transition.

(50) H.-J.Werner, *Mol. Phys.* **1996**, *89*, 645.
(51) Atanasov, M. *Inorg. Chem.* **1999**, *38*, 4942.

Summary

This study has shown that the existing repertoire of quantum chemical methods has become suitable to investigate heavy transition element systems in closed shell as well as in open shell configurations. The scalar relativistic effects can be incorporated either by using quasirelativistic pseudopotentials (G98, MOLPRO98) or the ZORA scalar relativistic option within ADF. Not only are existing experimental data such as vibration frequencies and absorption energies well reproduced, but the results also suggest the stability and thus isolability of certain yet unknown states such as the OsS_4^- and OsS_4^{2-} ions. In a next necessary stage of calculations, the effects of the environment will have to be considered, which should be essential for anionic systems.

Acknowledgment. This research was supported by Deutsche Forschungsgemeinschaft, Volkswagenstiftung, and Fonds der Chemischen Industrie. Also, financial support from the Ministry of Education of the Czech Republic (OC.D14.20) and from the Granting Agency of the Czech Republic (203/97/1048) is gratefully appreciated.

Note added in proof: A related study on FeO_4, FeO_4^-, and FeO_4^{2-} has recently appeared.[51]

IC990891F